## **CONFERENCE PRE-PRINT**

# NATURAL SMALL ELMS ACHIEVED AT LOW PEDESTAL COLLISIONALITY (<1) IN A METAL WALL ENVIRONMENT ON EAST

Y.F. WANG, G.S. XU, Q.Q. YANG, X. LIN, Q. ZANG, T. ZHANG, L. ZHANG, M.R. WANG, G.Z. JIA, N. YAN, R. CHEN, L. WANG
Institute of Plasma Physics, Chinese Academy of Sciences
Hefei, China
Email: yfwang@ipp.ac.cn

H.Q. WANG General Atomics San Diego, United States of America

X.Q. XU and N.M. LI Lawrence Livermore National Laboratory Livermore, United States of America

#### Abstract

Relatively low normalized pedestal collisionality (~0.66) has been achieved with low plasma density and high heating power on EAST, accompanied by large type-I ELMs. The amplitude of type-I ELMs is observed to increase with decreasing pedestal collisionality, which is consistent with the type-I ELM characteristic on other tokamaks. Natural small ELMs have been obtained at relatively low normalized pedestal collisionality (<1) with near double null configuration on EAST. Linear pedestal stability analysis suggests that the ballooning stability boundary significantly expands with the DN configuration, making the operational point move closer to the peeling stability boundary. The achievement of this small ELM regime has been found to be correlated to high poloidal beta, high ne,sep/ne,ped and double null configuration. Under the conditions of high plasma density and low heating power, large ELMs have been successfully mitigated by changing strike point location on the divertor target plate, accompanied by significantly enhanced separatrix density. This is correlated with a higher ionization source in scrape-off layer region when the strike point moves away from the divertor corner region, which is thought to provide a strong fuelling near separatrix and thus enhance the separatrix density. Linear pedestal stability analysis suggests that the operational point is located near the ballooning stability boundary. However, under the conditions of low plasma density and high heating power, large ELMs are not mitigated by changing strike point location. The separatrix density is nearly unchanged, which is thought to be due to the low edge fuel recycling under these conditions. Further work is needed to find key plasma parameters for small ELM regime access and to better understand the physical mechanism behind the small ELM regime.

# 1. INTRODUCTION

Future fusion tokamak reactors will be operated at low pedestal collisionality with high auxiliary heating power. For example, the pedestal collisionality will be  $\sim$ 0.01 for ITER [1] and  $\sim$ 0.2-0.5 for CFETR [2]. The normalized plasma energy loss during each type-I ELM burst has been found to increase with the decreasing pedestal collisionality and estimated to be  $\sim 20\%$  in ITER [1], which is thought to be unacceptable. Natural small or no-ELM H-mode regimes compatible with low pedestal collisionality have been developed so far as a solution to large ELM control, such as the grassy ELM regime and QH-mode. As a promising scenario in future fusion reactors, the grassy ELM regime has been extensively investigated, demonstrating the compatibility of this regime with good energy confinement, steady-state operation, low rotation, high density, high bootstrap current fraction and radiative divertor. The high frequency and small amplitude ELMs in this regime exhibits strong capability in the exhaust of high-Z impurities, making this regime suitable for operation in full metal wall environment in future fusion reactors. On DIII-D, we have observed a natural grassy ELM regime at low pedestal collisionality (~0.15). It has been found that a low density pedestal gradient after raising the heating power could help achieve this regime. On EAST, we have also achieved a natural grassy ELM regime, but at relatively higher pedestal collisionality (>1). To further develop the predictive capability towards future fusion reactors, it's necessary to extend the small ELM regime to lower pedestal collisionality on EAST and improve our understanding on the small ELM regime. By scanning the pedestal collisionality based on a small ELM discharge on EAST, BOUT++ simulation suggests with a low pedestal collisionality, the small ELMs can be still achieved on EAST. In this paper, the achievement of natural small ELMs at relatively low pedestal collisionality (<1) on EAST will be reported. EAST is a fully superconducting medium-size tokamak with modern divertor geometry. Various auxiliary heating and current drive methods, such as Lower Hybrid Wave (LHW), Ion Cyclotron Resonance Heating (ICRH), Electron Cyclotron Resonance Heating (ECRH) and Neutral Beam Injection (NBI) are applied

to enhance the plasma performance on EAST. In 2021 EAST campaign, the lower divertor has been upgraded to a tungsten divertor characterized by a right-angled corner at the outer divertor target plates, allowing for high performance long-pulse operation with stationary heat exhaust up to 10 MW/m<sup>2</sup>. Diagnostics for measurement of pedestal profiles have developed on EAST and can provide critical information for edge plasma analysis.

## 2. EXPERIMENTAL RESULTS

According to the definition of normalized pedestal collisionality, it is related to electron density ne and electron temperature T<sub>e</sub> at pedestal top and safety factor at the 95% normalized poloidal flux surface q<sub>95</sub>. To achieve a low pedestal collisionality, the plasma density has been reduced as low as possible by turning off gas-fuelling. The lower outer strike point is also located on the horizontal target plate near the pump port to improve particle pumping rate, facilitating a lower plasma density. The low plasma density also facilitates a high plasma temperature. However, the plasma density can't be too low because the shine-through power loss of NBI would increases as density deareases. At the same time, high heating power has been applied to obtain a high pedestal temperature. To improve the heating efficiency of electron cyclotron resonance heating (ECRH), toroidal magnetic field B<sub>T</sub>~2.5T has been applied with a medium q<sub>95</sub>~5-6. Figure 1 shows time trace for a typical discharge with low pedestal collisionality achieved by turning off gas fuelling with high heating power on EAST. This discharge is obtained at Ip=500kA, q95~4.9, lower single null (LSN) divertor configuration, in unfavourable B<sub>T</sub> direction, with auxiliary heating power including 1MW 4.6GHz LHW, ~1.45MW ECRH and ~5.2MW NBI. As shown in the figure, large ELMs (ELM frequency  $f_{\rm ELM}$ ~80Hz) appear after access to the H-mode phase, and then the ELM amplitude decreases as heating power increases. The gas fuelling is turned off from 3.5s and plasma density gradually decreases accompanied by an increase in ELM amplitude with  $f_{\rm ELM}$  decreases from 140Hz to 100Hz. The ELM amplitude is very large and we can clearly see that the plasma stored energy is reduced when the ELM bursts. The plasma stored energy remains ~230kJ during the heating power flat top phase.

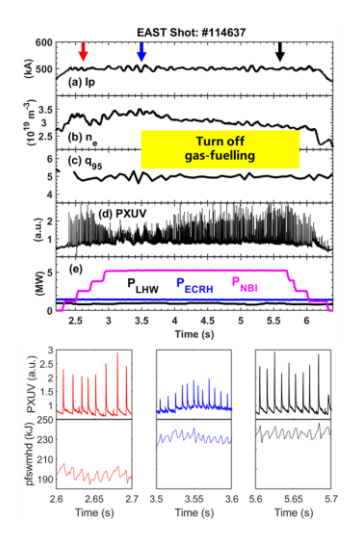


Figure 1. Low pedestal collisionality has been achieved by turning off gas fuelling with high heating power on EAST

Figure 2 shows the edge profiles before and after turning off the gas fuelling. We can see that after turning off the gas fuelling, from the blue case to the black case, the whole density profile in the edge region decreases, The temperature inside the pedestal top increases. So, the pressure profile inside pedestal top changes small. While the separatrix pressure deceases, leading to a higher pressure gradient and a higher edge peak current density. The ion temperature in the core also increases. The Er given by DBS shows that the separatrix Er is near 0, suggesting that the radial position of ne profile is reasonable. The pedestal width for both cases are shown to be consistent with previous pedestal width scaling on EAST. Based on edge profiles, we obtain the pedestal collisionality and normalized ELM energy loss. After turning off the gas fuelling, relatively low pedestal collisionality ~0.66 is achieved and the normalized ELM loss increases as pedestal collisionality decreases, this is consistent with previous studies on type-I ELMs on other tokamaks. Figure 3 shows the ELITE results. Before turning off gasfuelling, the operational point is located near the ballooning boundary. After turning off gas-fuelling, the operational point moves to higher alpha and j value. The ballooning boundary also expands because the ion diamagnetic frequency increases. As a result, the operational point moves to near the corner of the PBM boundary, providing trigger for larger ELMs. After turn off gas fuelling, the most unstable toroidal mode number changes

from 35 to 20. The right figure shows the BALOO code results for these two cases. We can see before turning off gas-fuelling, the ideal ballooning mode is more unstable at the pedestal foot region, this may help drive particles and heat transport, preventing larger ELM bursts.

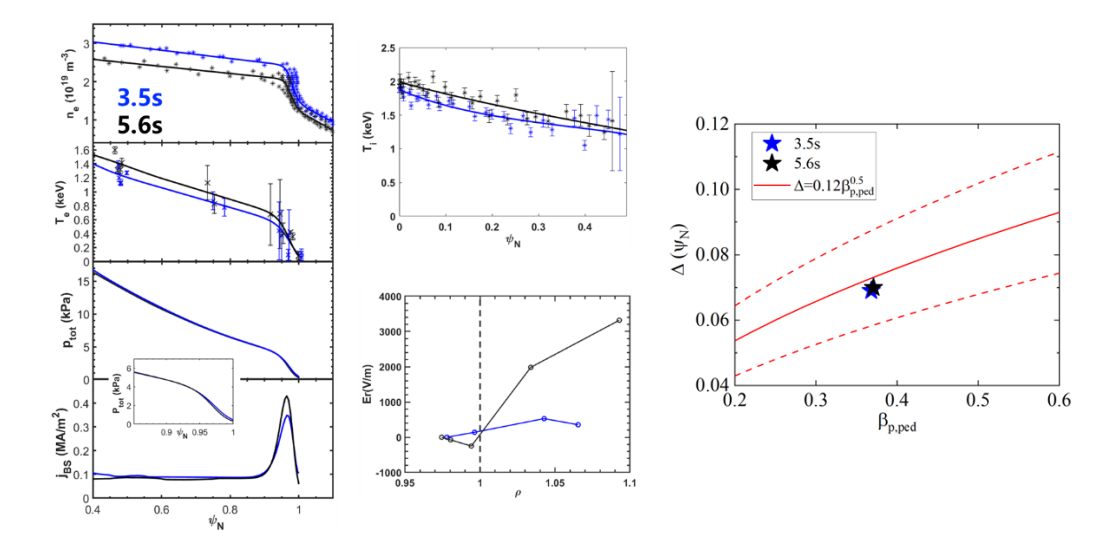


Figure 2. Edge profiles before and after turning off the gas fuelling are shown, including electron density ne measured microwave reflectometry, electron temperature Te measured by Tomson Scattering, total pressure ptot, bootstrap current  $j_{BS}$  calculated with the Sauter model, ion temperature Ti measured by the XCS diagnostic, Er profile provided by DBS diagnostic based on the measured ne profile. Comparison of the measured pedestal width with previous pedestal width scaling on EAST is also shown.

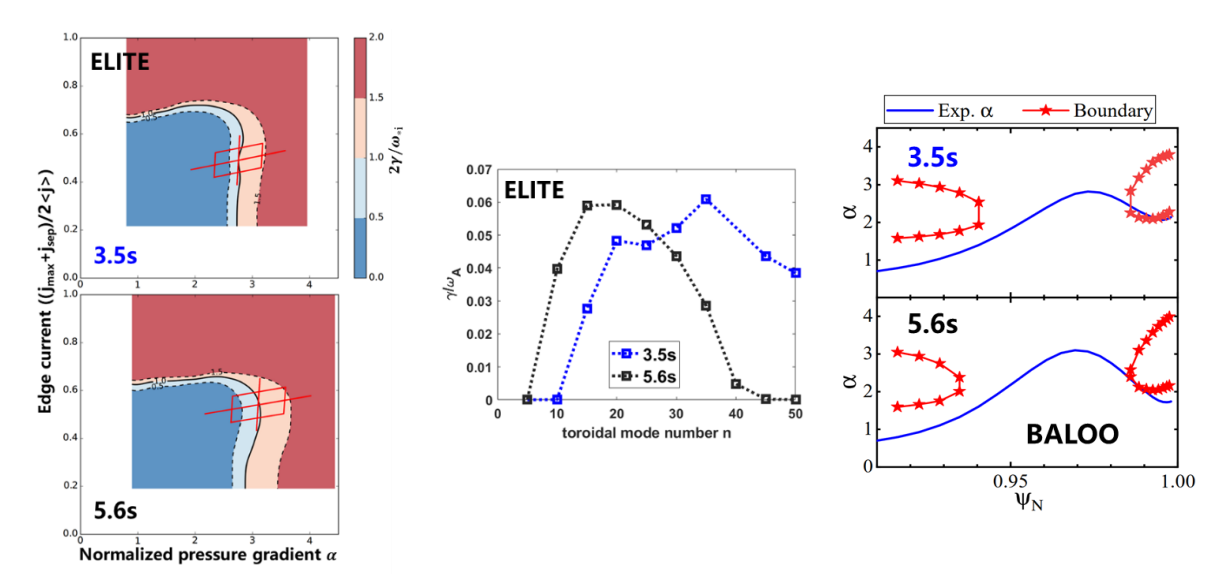


Figure 3. The stability diagram obtained with the ELITE code, the normalized growth rate of different toroidal mode numbers and the pedestal ideal ballooning mode instability calculated with the BALOO code are shown for the equilibria before and after turning off the gas fuelling.

We have also changed the plasma shape in our experiment. Figure 4 shows two discharges with different dRsep. The blue one is near DN configuration, and the red one is LSN configuration. q95 is also different because the plasma shape is changed. The plasma current, total stored energy, li, plasma density, source heating power are all the same in both discharges at 3.2s as shown with the yellow mark in the figure. We can see that with near DN configuration, the ELM frequency is 600Hz much higher than the LSN configuration. The ELM size in the DN configuration is also expected to be smaller. However, the temporal resolution of the total stored energy signal is not high enough to give the high-frequency ELM energy loss. Figure 5 compares edge profiles of these two discharges with different plasma shapes. We can see that with near DN configuration, the n<sub>e,sep</sub> and n<sub>e,ped</sub> are both higher. The temperature inside pedestal top region doesn't show obvious change. The pressure profile inside the

pedestal top region also doesn't shows obvious change. This is consistent with that the plasma total stored energy is almost the same in both cases. The figure also shows the pedestal stability diagram obtained with the ELITE code. We can see that for the DN configuration, the ballooning boundary significantly expands compared with the LSN configuration. and the operational point is located near the peeling boundary.

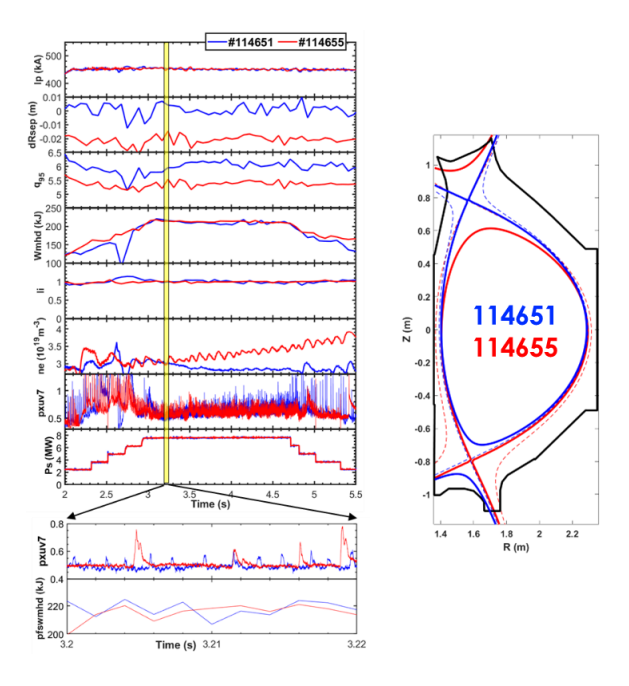


Figure 4. Small ELMs at relatively low pedestal collisionality (<1) have been achieved with near-DN configuration on EAST.

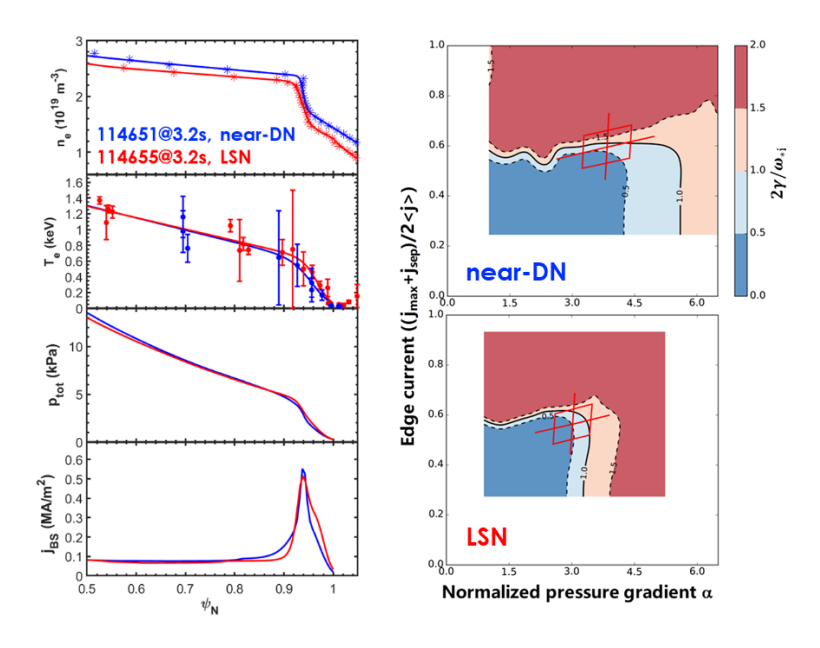


Figure 5. Edge profiles in near-DN and LSN configurations are shown, including electron density  $n_e$  measured microwave reflectometry, electron temperature  $T_e$  measured by Tomson Scattering, total pressure  $p_{tot}$ , bootstrap current  $j_{BS}$  calculated with the Sauter model. The pedestal stability diagrams obtained with the ELITE code are also shown.

To study the impact of plasma shape on the linear pedestal stability, we numerically exchange the plasma shape in both cases. Figure 6 shows the edge pressure profile and bootstrap current density profile. The solid lines represent the experimental profiles. The red dashed line represents the profiles calculated based on profiles from red solid case, but with plasma shape from blue case. For the DN configuration, at the rho value, the  $\psi_N$  is larger in the DN compared with LSN. This leads to a higher pressure gradient and a higher peak edge current density in

the red dashed case compared with the red solid case, making the operational point moves to higher  $\alpha$  and j value. The ballooning boundary also expands, which is thought to be because the ion diamagnetic frequency increases. So as a result, with a DN configuration, the operational point moves closer to the peeling boundary. For the blue dashed case, the result is similar.

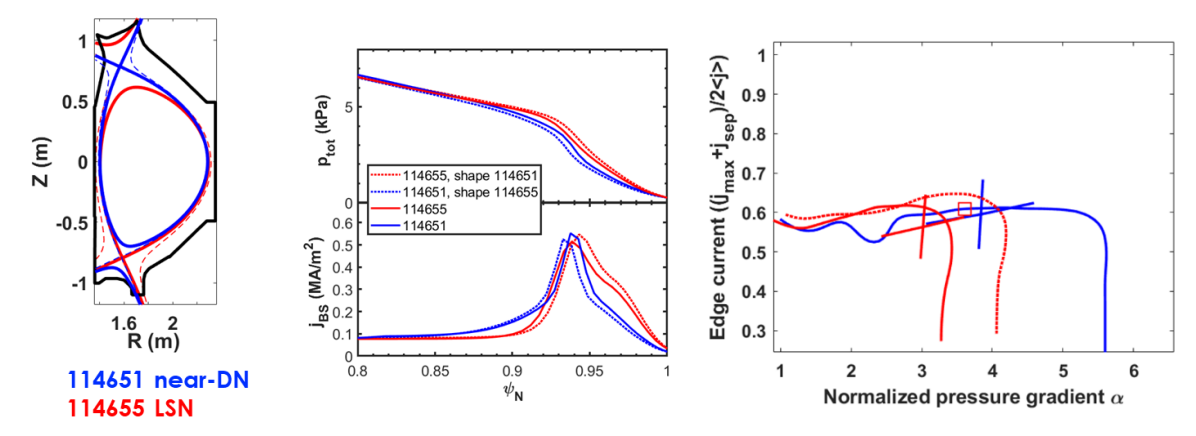


Figure 6. The plasma shapes used for numerical analysis, edge pressure profiles and bootstrap current density profiles calculated with different plasma shapes and the stability diagrams obtained with the ELITE code are shown.

Figure 7 shows a small ELM discharge with good energy confinement performance achieved at relatively low pedestal collisionality on EAST. During this discharge, a natural small ELM phase with ELM frequency ~ 600Hz is achieved, which only lasts for 200ms and then large ELMs appear. To understand the ELM behavior, this discharge is divided into 4 phases as shown in figure 8. In phase 1, large ELMs are triggered at low plasma density as NBI heating power increases. After further raising NBI heating power, large ELMs are replaced by natural small ELMs in phase 2. The increase in poloidal beta is thought to facilitate the mitigation of large ELMs. In phase 3, the separatrix density appears to decrease gradually, leading to a lower ne,sep/ne,ped and a higher density gradient. This would help trigger large ELMs. In phase 4, the pedestal top density gradually decreases because the gas fuelling is turned off, resulting in an increase in ne,sep/ne,ped and pedestal top temperature. The ELMs in this phase are mixed by grassy ELMs and type-I ELMs as shown in figure 9. During the small ELM phase, the density pedestal collapse during each ELM burst, while the temperature pedestal shows very small changes. As a result, the temperature at the pedestal top keeps increasing until large ELM occurs. As pedestal top temperature increases, a broadband frequency fluctuation has been observed during the inter-ELM phase as shown in figure 10 and figure 11, suggesting that this fluctuation is strongly correlated with low pedestal collisionality.

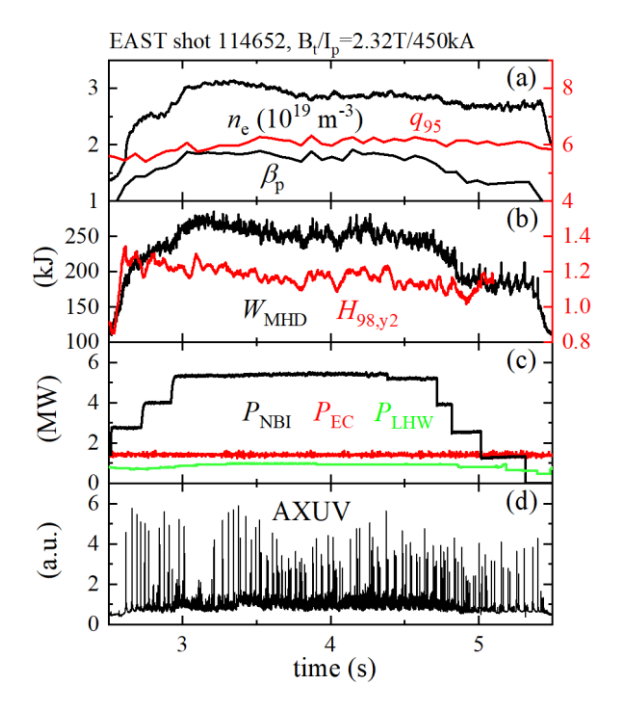


Figure 7. A typical discharge at relatively low pedestal collisionality with good energy confinement on EAST

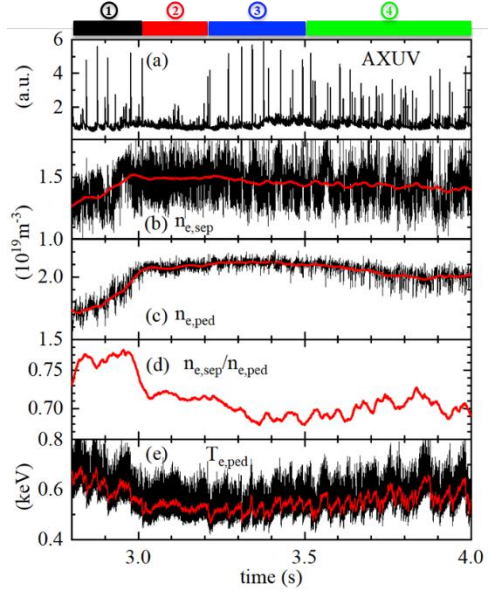


Figure 8. Time traces for (a) AXUV signal, (b) separatrix density, (c) pedestal top density, (d)  $n_{e,sep}/n_{e,ped}$  and (e)  $T_{e,ped}$  are shown.

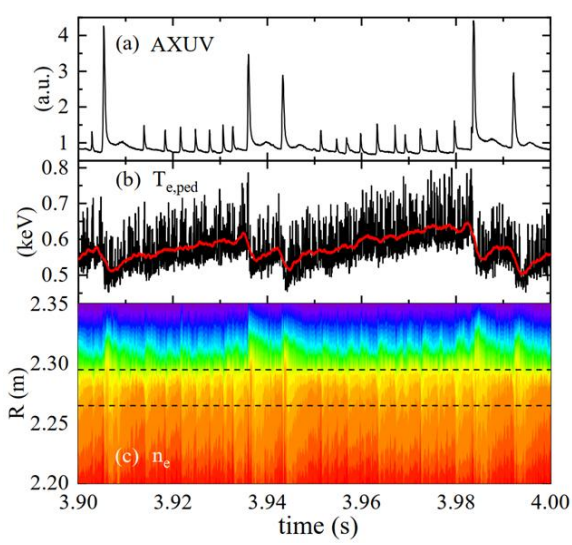


Figure 9. Time traces for (a) AXUV signal, (b) pedestal top temperature, (c) edge electron density profile in the mix-ELM phase 4 are shown.

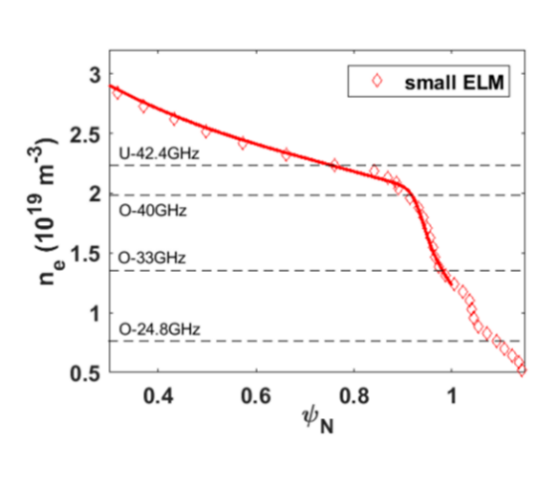


Figure 10. The edge electron density profile in small ELM phase is shown with cutoff density marked.

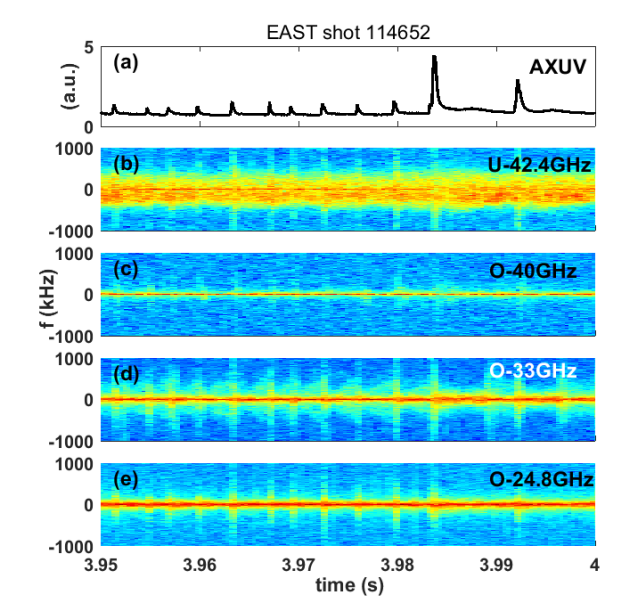
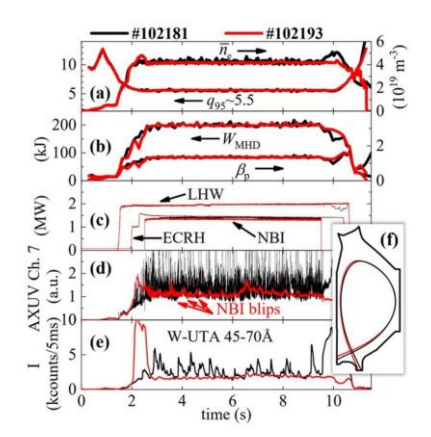


Figure 11. Time traces for (a) AXUV signal, (b) pedestal top temperature, (c) edge electron density profile in the mix-ELM phase are shown.

Large ELM control has been performed through actively changing fuel recycling by moving the strike point location on the lower tungsten divertor target plate as shown in figure 12 [3]. It has been demonstrated that the mitigation of large ELMs is strongly correlated with the significant increase in separatrix density (figure 13), which is thought to be attributed to a higher ionization source in the scrape-off layer (SOL) region by SOLPS-ITER simulation (figure 14). The high ionization source in the SOL region is believed to provide a strong fuelling effect near the separatrix and thus raise the local density, which is considered an important reason for triggering ballooning instabilities near the separatrix and achieving small ELMs. However, the separatrix density doesn't change much by changing strike point location at low pedestal collisionality and large ELMs are not mitigated as shown in figure 15 and figure 16.



4 Θ Θ 1 102181@5.228 102193@5.228 0.6 0.8 1.0 Ψ<sub>N</sub>

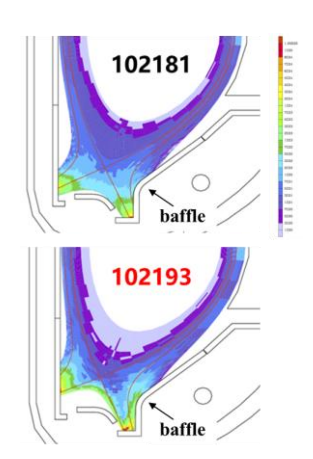
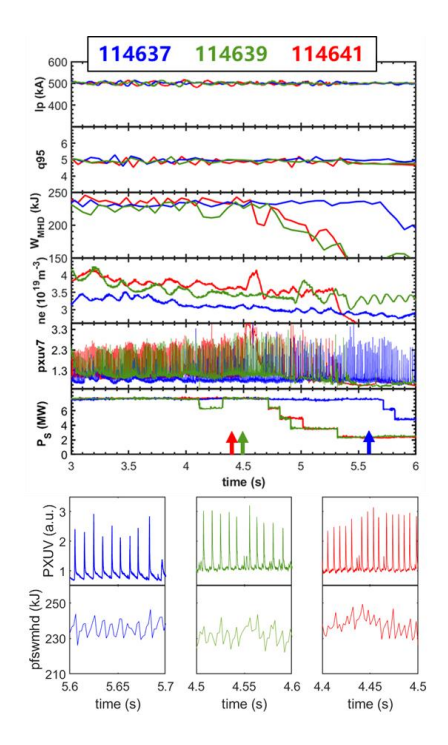


Figure 12. Large ELMs are mitigated by changing strike point location at high collisionality.

Figure 13. Comparison of edge density profile with different strike point locations

Figure 14. 2D ionization source for different strike point locations simulated by SOLPS-ITER



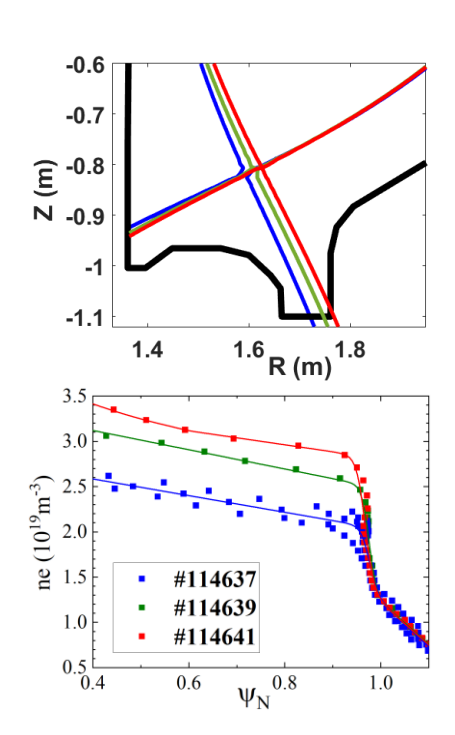


Figure 15. The basic information of three discharges with different strike point locations at low pedestal collisionality are shown.

Figure 16. Strike point locations (upper) and edge density profiles (bottom) in three discharges are shown.

# 3. SUMMARY AND DISCUSSION

Natural small ELMs have been achieved at relatively low pedestal collisionality (<1) with good energy confinement on EAST. Several factors are thought to be important to get access to this small ELM regime. The natural small ELMs appear after raising heating power, suggesting high poloidal beta facilitates the small ELMs. The strong Shafranov shift at high poloidal beta squeezes the flux surfaces on the low-field side which reduces the flux-surface averaged current density. In addition, high  $n_{e,sep}/n_{e,ped}$  could lead to lower pressure gradient and also lower peak edge current density, which would also prevent triggering of large ELMs. With double null configuration, the ballooning stability boundary significantly expands. This makes the pedestal operational point move closer to the peeling stability boundary and away from the corner of peeling-ballooning boundary, preventing large ELMs. A broadband frequency fluctuation has been observed at low pedestal collisionality in the pedestal foot region in inter-ELM phase, which is different from the coherent modes usually observed at high collisionality on EAST. At high collisionality, the separatrix density can be significantly enhanced by moving

#### IAEA-CN-316/EX-E/P4-3207

strike point location due to an increase in fuelling from an elevated ionization source in the SOL, leading to large ELMs mitigation. However, the separatrix density doesn't change much by moving strike point location at low pedestal collisionality and large ELMs are not mitigated.

## **ACKNOWLEDGEMENTS**

This work was supported by the National Magnetic Confinement Fusion Energy Program of China under Grant No. 2019YFE03030000, 2022YFE03020004 and 2024YFE03270400 and the Strategic Priority Research Program of Chinese Academy of Sciences under Grant No. XDB0790101 and the National Natural Science Foundation of China under Contract No. 12005263.

## REFERENCES

- [1] WANG, Y.F. et al., Grassy ELM regime at low pedestal collisionality in high-power tokamak plasma, Nucl. Fusion 61 (2021) 016032.
- [2] LI, Z.Y. et al., Ideal MHD stability and characteristics of edge localized modes on CFETR, Nucl. Fusion 58 (2018) 016018
- [3] WANG, Y.F. et al., Dependence of ELM instability on separatrix density in EAST long-pulse H-mode plasmas, Nucl. Fusion 64 (2024) 126017.